Quality Monitoring in Robotised Welding using Sequential Probability Ratio Test

Stefan Adolfsson[1], Ali Bahrami[2], Ingvar Claesson[3]

June 27, 1996

[1]Department of Signal Processing, University of Karlskrona\Ronneby and Department of Production and Materials Engineering, Lund University

[2]Department of Production and Materials Engineering, Lund University and Technology Center of Kronoberg, Vaxjo

[3]Department of Signal Processing, University of Karlskrona\Ronneby

Abstract

This paper addresses the problem of automatic monitoring the weld quality produced by robotised short arc welding. A simple statistical change detection algorithm for the weld quality, recursive Sequential Probability Ratio Test (SPRT), is used. The algorithm may equivalently be viewed as a cumulative sum (CUSUM) - type test. The test statistics is based upon the variance of the amplitude of the weld voltage. The performance of the algorithm is evaluated using experimental data. The results obtained from the algorithm indicate that it is possible to detect changes in the weld quality automatically and on-line.

Chapter 1

Introduction

Background

An ongoing process of automatization of the production lines is implemented in industry in order to reduce production costs. Automatization of quality control should be seen as part of the cost reduction, as also should be quality control of welding.

Monitoring systems of weld parameters, such as ADM III, Arc guard, and Weldcheck are commercially available. [?, ?]. They all work in a similar way; voltage, current and other process signals are measured, presented and compared with preset nominal values. An alarm is triggered when the difference from preset values exceeds a given threshold.

In the field of short arc welding of steel, both physical analysis of the welding process [?, ?] and statistical analysis of measured welding signals have been made [?, ?, ?].

The objective of the present paper is to detect changes in weld quality automatically in short arc welding using signal processing methods.

In order to achieve an uniform weld quality the welding process must be stable. The process stability, i.e the characteristics of the welding should not change in an uncontrolled manner. Experiments have shown that optimal stability occurs when the number of short circuits per seconds are at their maximum [?, ?].

Thus, a suitable parameter for detection of changes in the weld quality, is the variance of the amplitude of the weld voltage. This parameter is used to form a test statistics and this in its turn is fed into a recursive Sequential Probability Ratio Test (SPRT) algorithm [?]. The algorithm may equivalently be viewed as a cumulative sum (CUSUM) - type test. The SPRT is optimal in the sense that it minimizes the worst mean delay for detection given a specified probability of false alarm [?]. In addition, storage and computational requirements for the recursive SPRT are less as compared to fixed sample-size tests.

The paper is organized as follows. Section 2 describes some experiments. Changes in the weld quality is provoked in weldings in a controlled way while the weld voltage and current from this process are monitored. Some changes of the the variance of the amplitude of the weld voltage during a weldingpass are observed. Section 3 deals with the design of the recursive SPRT algorithm. The section concludes by showing how the algorithms are used to detect defects in the weld joint. Section 4 deals with tuning and estimation of parameters used in the algorithm. Robustness of the proposed algorithm is also considered. The recursive SPRT is then evaluated using experimental data. The paper concludes with a discussion of the performance of the method in section 5.

Chapter 2

Welding technology

2.1 Short arc GMA welding

The GMA welding process employs a consumable wire electrode passing through a copper contact tube. See figure 2.1. Electric current supports an arc flowing from the end of the electrode to the work piece. The electrode is melted by resistive heating, and heat from the arc. The region surrounding the weld puddle is purged with shield gas to prevent oxidation and contamination of the weld joint [?, ?, ?, ?].

Figure 2.1: A schematic illustration of equipment for short arc GMA welding. The electric current of the weld process is denoted I. The internal resistance and indictance of the welding source is denoted R_i and L_i respectively. The resistance of the wire electrode stick-out, i.e the part of the electrode between the contact tube and the arc, is denoted R_e. The length of the electrode stick-out and the arc length are denoted ℓ_e and ℓ_a respectively. The voltage over the wire electrode stick-out is denoted U_e. The voltage between electrode tip and work piece is called the arc voltage and is denoted U_a

The advantage of the short cicuiting welding is that the mean current, and thus the average heat input to the work piece, is lower than in direct current (DC) GMA welding. Due to the smaller heat transfer, it is possible to weld thinner plates with short arc GMA than with DC GMA welding.

Figure 2.2: A schematic illustration of the weld voltage and current in short-cicuiting welding. T_a and T_s denote the peak pulse time and background pulse time respectively; and I_p and I_b denote the peak current and background current respectively.

To limit the heat input to the work piece, the open circuit voltage is set at a low value compared to (DC) GMA welding. The electrode is molten and a small droplet is developed at the electode tip. This part of the cycle is denoted 'arc time' and represented by T_a. [?, ?, ?].

During short cicuiting time, T_s, the voltage will decrease to almost zero volt and the current will increase to its maximum value. At this stage the arc will extinguish and a droplet is detached and transferred to the work piece. The main force for detaching a droplet and transferring it, is the electromagnetic force induced by the current [?]. After the transferring of the droplet the arc is re-ignited and the cycle starts over again.

The weld voltage U_w, arc voltage, U_a, and the voltage over the wire electrode stick-out, U_e are related by

$$U_w = U_a + U_e, \tag{2.1}$$

2.2 Optimal welding conditions

In order to produce weld joints with uniform weld quality it is desirable that the welding process is stable. Inter alia should the metal transfer from the electrode wire to the work piece occur under stable and regular conditions as possible. Experiments have shown that optimum stability occurs when the number of short circuits per second are at their maximum given that the short circuit time exceeds 1 ms, see figure 2.3. Thus, the welding process is said, in this report, to operating under optimal welding conditions when the number of short circuits per second are at their maximum. Deviation from the optimal condition leads to a greater probability of spatter, uneven weld bed and other fusion defects. In this case the welding process is said to operate under non-optimal condition.

Figure 2.3: Short arc transfer frequency

The number of short circuits per second is controlled by the open circuit voltage V_{oc}. When the open circuit voltage is set at greater value than under optimal condition, the metal transfere will either be globular or spray. Globular metal transfer is deemed to be unstable, while spray transfer is considered as a naturally stable process but not suitable for welding thin plates.

For the three main main metal transfer modes, short-circuiting, globular and spray, there is a correlation between the waveform and mode of metal transfer. It can be seen, moving from short-circuiting to globular and spray transfer, that the variation range on the welding current and voltage wavwform reduces. The minimum and maximum current approaches the mean welding current, See figur 2.4 part a-c.

Figure 2.4: Waveforms for metal transfer modes

When the open circuit voltage is set at lower value lower than under optimal condition, the heat to melt down the electrode during arc time is not sufficient. The electrode has, then, to melt down during short-circuiting time. Since the short-circuiting time increases so will the peak current and the variation range on the weld current increases compared to normal welding condition. In this case the variation range on the weld current increases but the variation range on weld voltage waveform decreases.

Thus, the developed algorithm in this report is based on the hypotheses that the variance or the AC power decreases when the welding process not work under optimal condition.

Chapter 3

Experiments

3.1 Aim of the experiments - provoke non optimal welding conditions

The aim of the experiments is to provoke non optimal welding conditions in controlled manner while monitoring the weld voltage and current from the process. Non optimal welding condition was provoked using a T-joint where gaps have been cut out in the standing plate, see figure 3.1 part c. This specimen is denoted a 'T-joint with step disturbance'. During the step disturbance the welding process is operating under non optimal condition. A second specimen shown in parts a and b is a T-joint with the standing plate in perfect contact with the laying plate. This specimen was used to produce normal or reference weldings and is thus denoted a 'reference T-joint'. During normal welding the welding process is assumed to operate under optimal welding condition.

The specimens were each comprised of two rectangular $200 \times 10 \times 3$ mm plates of mild steel SS 1312. For the T-joint with step disturbance, the dimension of the gap was 2×50 mm. See figure 3.1 part c.

Figure 3.1: Steel T-joints provoking defects in weld joints. a) Reference T-joint, front view b) Reference T-joint, side view c) T-joint with step disturbance, front view

3.2 Instrumentation

The experimental setup is made up of a welding power source, a Motoman robot carrying a welding torch, a positioner, a welding table and instrumentation for recording weld voltage and current, see figure 3.2. The welding torch is fixed in at angle of 45 degrees to the welding table. The distance between the contact tube tip and the plate is 11 mm.

Figure 3.2: The experimental setup is made up of welding power source a Motoman robot carrying a welding torch, a positioner and instrumentation for recording welding voltage and current.

The weld voltage is measured between an electrode applied to the contact tube and a reference electrode screwed into an aluminum plate which serves as an insulated welding table [**?**]. The current is measured with a current sensor, LEM Module LT 500-S, equipped with a transformer. The sensor is mounted around the return conductor. The sampling frequency is 8.192 kHz, and the resulting lowpass filter has a cut frequency of 1.0 kHz. The data are then transferred for permanent storage to a personal computer.

Two different commercial welding equipment, Migatronic BDH S50 and Kemppi P500, were used for the experiment. The wire feed rate was measured to be approximately $113-120$ mm/s and the nominal welding speed was set at 10 mm/s. The filler wire material used in the experiment was ESAB OK 12.51 with a diameter of 1.0 mm. The shielding gas used was Atal: $80\%Ar/20\%CO_2$. The flow rate of shielding gas was set at 15 l/min.

3.3 Measurments

3.3.1 Experimental procedure

Before starting to measure, the specimen is positioned on the aluminum plate and fixed by a fixture. Since the torch is attached to the Motoman robot, the welding speed is determined by the speed of the robot. The weld speed is set at 8, 10 and 12mm/s, respectively. The robot is started manually by the operator, who then starts the weld source. This in turn sends a trigger signal to the acquisition system, which starts to record data. For the T-joint with step disturbance, the operator starts the weld sex centimeter before the cut. See figure 3.1. For the reference T-joint, the weld is started 2 cm from the edge side. T length of the weld joint is approximately 13 cm.

3.3.2 Recorded data

For all measurements, 2 channels were used: one for the weld voltage and one for the weld current. 90 experiments in total were conducted during four days. Fifty seven experiments were conducted for the T-joint with step disturbance and 33 reference T-joint. The recording time of the measured signals was 15 s for step disturbance, reference and ramp disturbance respectively. There were 34 burn-throughs in all in the weld joints produced; 11 burn-throughs in the T-joint with step disturbance; 23 burn-throughs in the T-joint with ramp disturbance, and no burn-throughs in the reference T-joints. As previously mentioned in the "Data acquisition system" section, the sampling frequency was 8.192 kHz, and the resulting lowpass filter had an upper frequency limit of 2 kHz.

Table 3.1: Total number of experiments

Welding Speed	Reference	Step
8 m/s	2	15
10 m/s	29	28
12 m/s	2	14
SUM:	33	57
Total:	90	

Table 3.2: Number of experiments conducted with Kemppi P500 - 960201

Welding Speed	Reference	Step
8 m/s	2	5
10 m/s	5	5
12 m/s	2	5

Table 3.3: Type and Number of experiments conducted with Kemppi P500 - 960304

Welding Speed	Reference	Step
8 m/s	0	10
10 m/s	11	10
12 m/s	0	9

Table 3.4: Type and Number of experiments conducted with Migatronic BDH S50 - 960325

Welding Speed	Reference	Step
8 m/s	0	0
10 m/s	7	7
12 m/s	0	0

Table 3.5: Type and Number of experiments conducted with Migatronic BDH S50- 960424

Welding Speed	Reference	Step
8 m/s	0	0
10 m/s	6	6
12 m/s	0	0

Chapter 4

Experimental Data Analysis

The purpose of this chapter is partly to confirm, by examination of the waveform of weld voltage and current, the assumption that the variance of the amplitude of the weld voltage and current decreases when the welding process deviviates from the optimal welding condition. Partly to investigate some parameters for monitoring short arc GMA welding such as, arc time, short arc time and short circuit peak current, which are suggested in published works in this field. Based on the performed investigation parmeters for monitoring are suggested.

4.1 Time domain analysis of measurment data

Figures 4.1 and 4.7 show photos of samples of a typical reference T-joints and a typical T-joints with step disturbance. Registrations of corresponding weld voltage and current are shown in figures 4.2, and 7. The position of disturbance in the weld joint is indicated at the bottom of respectively voltage diagrams. Corresponding measured parameters are shown in figures ?? to figures ?? and 4.10 to?? respectively.

Short arc transfer frequency

Figure ??,Figure 4.10 and Figure 4.20 part a, shows measured short circuit transfer frequency curve. During short-circuit time melted electrod materials are transfered to the work piece, see figur 2.2. When the metal transfer from the electrode wire to the work piece occur at regular intervals the probability of stable weld process is increased. The metal transfers are reflected in the weld voltage as almost zero voltage events of 2 ms in figure 4.3, figure 4.9 and figure 4.19. According to previous described hypothesis the number of short-circuit per second is expected to decrease when the welding process is disturbed. Figure 4.10 verify this assumption. In figure 2.2 it can be read of that the number of short-circuit per second shall be 100 when the welding process working under optimal conditions. In figure 4.10 is the number a bit greater but in broad outline verify the assumed hypothesis. During the step disturbance the number of short-cicuting decreases to almost half compared to when the welding process is working under optimal conditions. In figur 2.2 it can be read off that the process is working in globular mode, i.e. in the C area or in area A.

Weld voltage during arc time

To decide if the process is operating in area A, B, C or D the mean value for arc time voltage is calculated, see figure ??,figure 4.10 and figure 4.20 part a. If the arc time voltage is greater than arc time voltage under optimal welding condition then then process is operating in area C. If the reverse is true the process is operating in area A. Figure 4.10 shows that, if not apparently, that the process are in area A, stubbing in mode, during step disturbance which indicate that the electrode tip is not heated sufficient enough.

Arc time

Figure ??,figure 4.10 and figure 4.20 part d shows arc time and part e shows the overall trend of the arc time. Medianfilter of length 100 was applied to the estimated arc time sequence in part d.

In figur 4.10 part e the arc time has increased from 7 ms to 14 ms during step disturbance. This observation is in line with previous observation above. Compare figure 4.10 part a and figure 4.10 part e. Assume that the short-arc time is constant under optimal as well as non optimal condition and the arc time is redouble under nonoptimal condition then will the number of short-circuiting per second decrease to half as much.

Short-circuiting time

Figure ?? part b shows that the short-circuiting time inreases in mean from 2.2 ms under optimal condition to 2.8 ms during step disturbance. If the weld voltage is to low the energy in the arc is not sufficient to melt the electrode and form a droplet that is suited for short circuit that will occur next. When this happens, an excessive amount of time must be spent in the short circuit phase in order to generate the heat necessary to melt the electrode and releas the droplet.

Short circuit peak current

Figure ?? part d confirm the results in Figure ?? part b. When the short-circuiting time increases so do the short circuit current peak. Both of these figures suggest that larger droplet is detached from the electrode for each short-circuiting cycle.

Mean and variance

The variance of the amplitude of the weld voltage might be a suitable parameter for detection of changes in the weld quality. When the variance of the weld voltage is larger than the variance during optimal conditions spatter has occurred. When the variance of the weld voltage is less than the variance during optimal conditions the number of short circuits per second are not at their maximum, indicating that the welding process is disturbed.

The weld voltage is divided into k sections, with $N = 1024$ samples in each section. The AC power is calculated for each section. The estimated mean and variance is shown in figure ?? parta and b. Note the decrease in the variance during step disturbance, indicating no optimal stability.

Figure 4.1: *Reference T-joint: Photo of the a) front and b) rear side of a welded joint.*

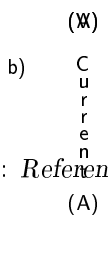

Figure 4.2: *Reference T-joint: a) Measured current and b) measured voltage.*

Figure 4.3: Reference T-joint: Close up view of a) measured weld voltage and b) weld current.

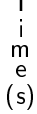

Figure 4.4: Reference T-joint: a) Measured short circuit transfer frequency curve and b) estimated mean voltage during arc time . c) Medianfilter of length 100 applied to the estimated mean voltage during arc time. d) arc time and e) medianfilter of length 100 applied to arc time sequence

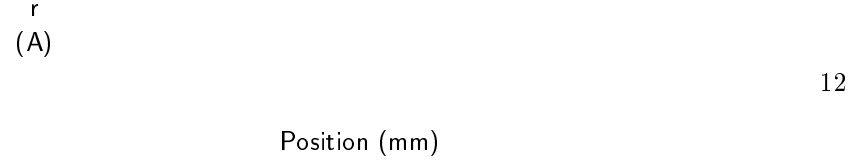

Figure 4.5: Reference T-joint: a) Measured short circuit current peak and b) medianfilter of length 100 applied to the short circuit current peak sequence in part a. c) Measured short-circuit time and b) medianfilter of length 100 applied to the short-circuit time current peak sequence in part a

Figure 4.6: Reference T-joint : a) Mean of the weld voltage and b) estimated variance of weld voltage. c) Mean of the weld current and d) estimated variance of weld current.

Figure 4.7: *T-joint with step disturbance No. 1 : Photo of the a) front and b) rear side of a welded joint.*

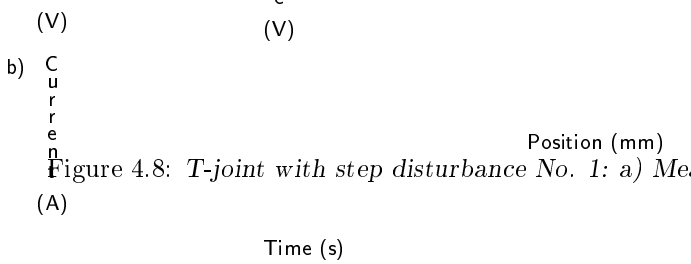

Figure 4.8: *T-joint with step disturbance No. 1: a) Measured current and b) measured voltage.*

Figure 4.9: During step disturbance: Close up view of a) measured weld voltage and b) weld current.

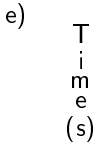

Figure 4.10: T-joint with step disturbance No 1: a) Measured short circuit transfer frequency curve and b) estimated mean voltage during arc time . c) Medianfilter of length 100 applied to the estimated mean voltage during arc time. d) arc time and e) medianfilter of length 100 applied to arc time sequency

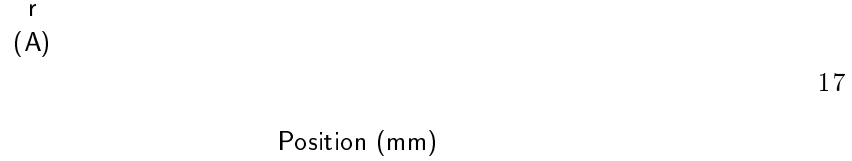

Figure 4.11: T-joint with step disturbance No 1: a) Measured short circuit current peak and b) medianfilter of length 100 applied to the short circuit current peak sequence in part a. c) Measured short-circuit time and b) medianfilter of length 100 applied to the short-circuit time current peak sequence in part a

r
(A)

Position (mm)

Figure 4.12: T-joint with step disturbance No 1: a) Mean of the weld voltage and b) estimated variance of weld voltage. c) Mean of the weld current and d) estimated variance of weld current.

4.2 Spectral domain analysis of measurment data

The spectra of recordings from normal welding condition can be compared with spectra of recordings during step disturbance in the search for relevant characteristics.

The weld voltage and current has been decimated to the samplings frequency 4092 kHz. The lowpassfilter used in the experiments has a cut-off frequency at 1 kHz, so the figures shows the spectra in the range 0-1 kHz. Estimation of the power spectral density of weld voltage and current is based on the periodograms method. This is described in Appendix A. The method is implemented with the command 'spectrum' in the MATLAB Signal Processing Toolbox [?]. With this command, the 8192 data samples are divided into 16 sections, with 1024 points in each section. The sections are detrended. In order to reduce the effect of spectral leakage, a Hanning data window is applied to the sections of the signal prior to computing the periodogram. To lower the variance of the estimate, the modified periodograms of the sections of the signal are averaged 95 % confidence interval is also calculated and plotted by the routine.
The result of the power estimation of the weld voltage and current for normal weld of a reference T-joint, and for a welding a T-joint with step, disturbance is shown in figure 4.13 part a - d. A visual comparison between the four power spectral densities shows that the main difference is above 70 Hz.

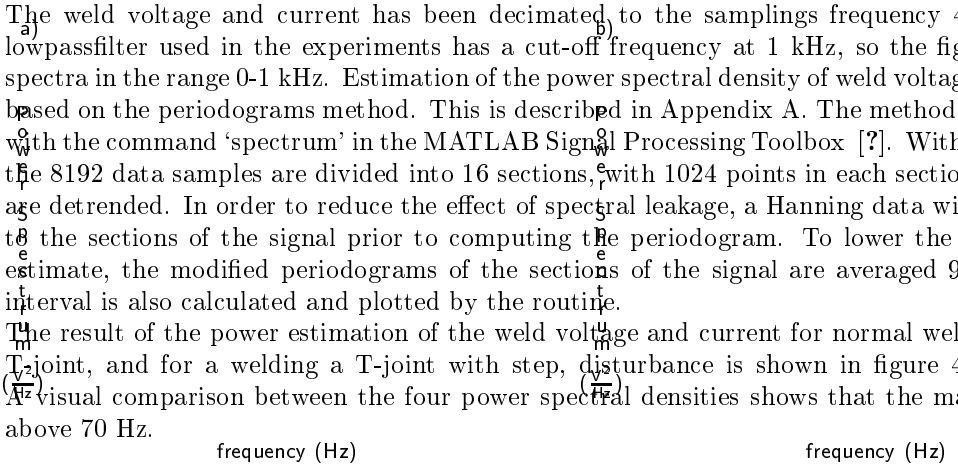

Figure 4.13: *Power spectral densities of a) the weld voltage from a reference T-joint during normal welding, b) the weld voltage from a T-joint with step disturbance during step disturbance, c) the weld current from a reference T-joint during normal welding and d) weld current from a T-joint with step disturbance during step disturbance. The dotted curve represents the* 95 % *confidence limits. Note the main spectral diffrence above 70 Hz*

4.3 Variance of filtered data

Filtering the data

Since the main difference in the power spectra of the weld voltage and current for normal welds, and for the welds during burn-through, occurs for frequencies over 70 Hz, the weld voltage and current is highpass-filtered with a discrete-time filter with the following specification [?]: The maximum pass-band ripple of the magnitude of the discrete-time filter, ≤ 0.1 dB. The minimum stop-band attenuation of the discrete-time filter is 60 dB. The stop band edge of the discrete-time filter is $f_1 = 50$ kHz. The pass-band edge of the discrete-time filter is $f_2 = 80$ Hz. This filter was designed with an elliptic filter of an order 8 in MATLAB, Signal Processing Toolbox [?]. The magnitude response of the elliptic filter is shown in figure 4.14.

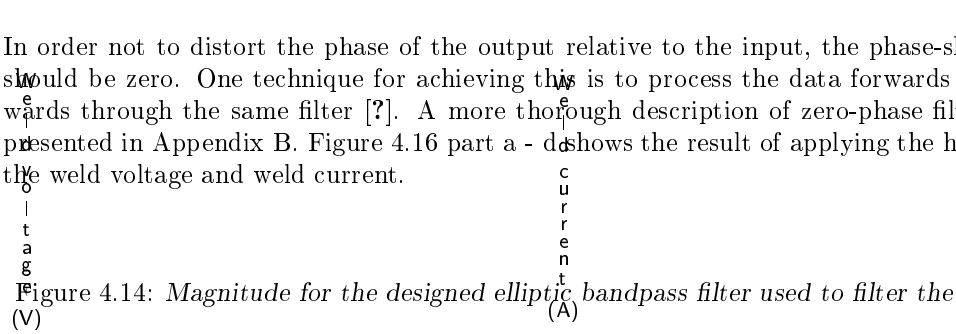

Figure 4.14: *Magnitude for the designed elliptic bandpass filter used to filter the weld voltage.*

In order not to distort the phase of the output relative to the input, the phase-shift of the filter should be zero. One technique for achieving this is to process the data forwards and then backwards through the same filter [?]. A more thorough description of zero-phase filter operation is presented in Appendix B. Figure 4.16 part a - d shows the result of applying the highpass filter to the weld voltage and weld current.

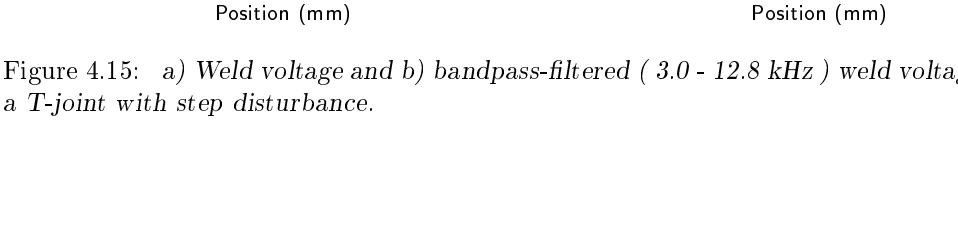

Figure 4.15: *a) Weld voltage and b) bandpass-filtered (3.0 - 12.8 kHz) weld voltage from welding a T-joint with step disturbance.*

Variance of filtered data

The variance of the amplitude of the filtered weld voltageand current might be a suitable parameter for detection of changes in the weld quality. When the variance of the weld voltage is larger than the variance during optimal conditions spatter has occurred. When the variance of the weld voltage is less than the variance during optimal conditions the number of short circuits per second are not at their maximum, indicating that the welding process is disturbed.

The weld voltage is divided into sections, with $N = 1024$ samples in each section. The variance for the filtered weld voltageand current is calculated for each section. The estimated mean and variance is shown in figure ?? part a and b. Note the decrease in the variance for both weld voltage and curret during step disturbance, indicating no optimal stability.
The estimated AC power is shown in figure 7.1 part b. Note the decrease in mean of the AC power estimate y_i during step disturbance, indicating no optimal stability. Same algorithm is also applied to the filtered weld current to obtain an estimate of AC power for filtered weld current.The estimated AC power is shown in figure 7.1 part b. Note the decrease in mean of the AC power estimate during step disturbance, indicating no optimal stability.

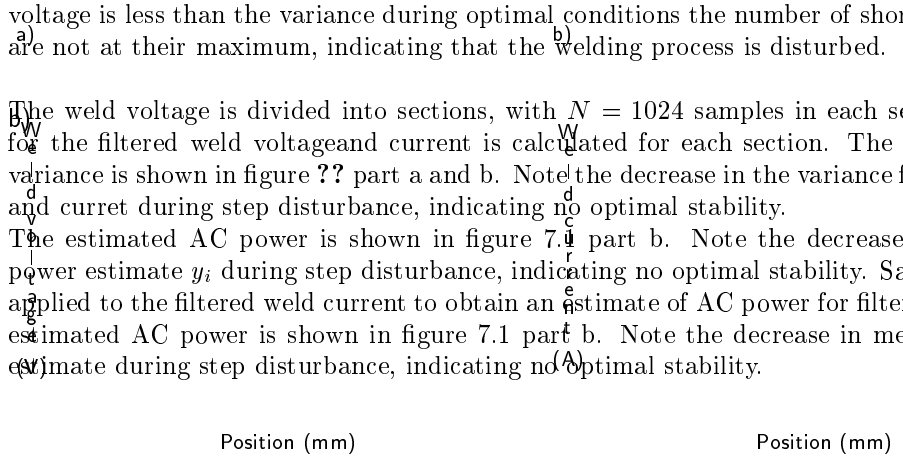

Figure 4.16: *a) ac power*

4.4 Selected parameters for monitoring short-arc GMA welding

The observations described above are typical of the weldings, though considerable deviations from the normal behavior can occur. The normal pattern for reference T-joint and T-joint with step disturbance are shown in figure 4.2 and figure ??, respectively. Deviation from the normal pattern for a T-joint with step disturbance are shown in figure ??. In which can be observed in figure ?? part a. The figure shows no decrease in number of short circuitings per second and b) no increase in maximum current, arc and short-circuiting time as well as maximum current.

Figure 4.17: *T-joint with a step disturbance No. 2. Photo of the a) front and b) rear side of a welded joint.*

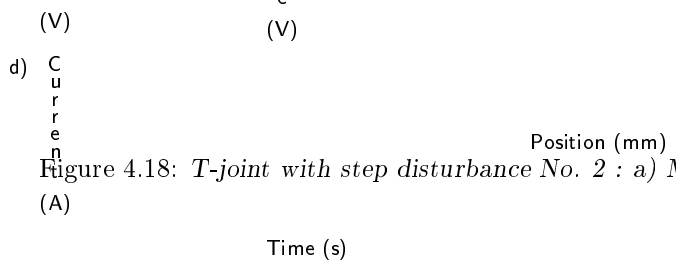

Figure 4.18: *T-joint with step disturbance No. 2 : a) Measured current and b) measured voltage.*

Figure 4.19: During step disturbance: c) Measured voltage and d) measured current.

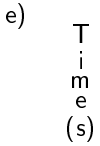

Figure 4.20: T-joint with step disturbance No 2: a) Measured short circuit transfer frequency curve and b) estimated mean voltage during arc time . c) Medianfilter of length 100 applied to the estimated mean voltage during arc time. d) arc time and e) medianfilter of length 100 applied to arc time sequency

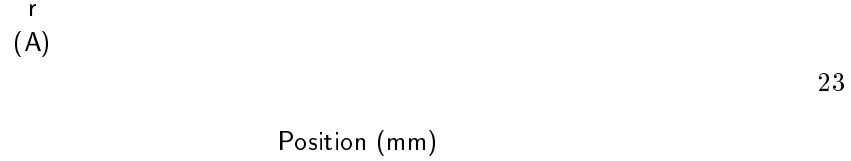

Figure 4.21: T-joint with step disturbance No 2: a) Measured short circuit current peak and b) medianfilter of length 100 applied to the short circuit current peak sequence in part a. c) Measured short-circuit time and b) medianfilter of length 100 applied to the short-circuit time sequence in part a

r
(A)

Position (mm)

Figure 4.22: T-joint with step disturbance No 2: a) Mean of the weld voltage and b) estimated variance of weld voltage. c) Mean of the weld current and d) estimated variance of weld current.

Chapter 5

Fault detection algorithm

When the variance of the weld voltage and current is larger than the variance during normal conditions spatter has occurred. When the variance of the weld voltage and current is less than the variance during normal conditions the number of short circuits per second are not at their maximum, indicating that the welding process is disturbed. To avoid confusion of ideas the variance of the amplitude of filtered the weld voltage and current is henceforth denoted AC power for weld voltage and AC power for weld current respectively.

The high pass filtered weld voltage is divided into k sections, with $N = 1024$ samples in each section. The AC power is calculated for each section and is given an index, i, defined by the position in the sequence. The AC power is estimated as follows:

$$y_i = \frac{1}{N-1}\sum_{p=1}^{N}(v_p - \overline{v})^2 \tag{5.1}$$

where v_p is the filtered weld voltage, N is the number of data points and $\overline{v}$ is the mean of the filtered weld voltage calculated as

$$\overline{v} = \frac{1}{N}\sum_{l=1}^{N} v_l \tag{5.2}$$

The estimated AC power is shown in figure 7.1 part b. Note the decrease in mean of the AC power estimate y_i during step disturbance, indicating no optimal stability. The sequence $\mathbf{y} = (y_0, y_1, \ldots y_k)$ is assumed to be identical, independent and Gaussian distributed with mean value μ and constant variance σ^2.

Same algorithm is also applied to the filtered weld current to obtain an estimate of AC power for filtered weld current.The estimated AC power is shown in figure 7.1 part b. Note the decrease in mean of the AC power estimate y_i during step disturbance, indicating no optimal stability. The obtained sequence sequence $\mathbf{y} = (y_0, y_1, \ldots y_k)$ is also assumed to be identical, independent and Gaussian distributed with mean value μ and constant variance σ^2.

Let $\mathbf{y} = (y_0, y_1, \ldots y_k)$ denote a random sample of scalar random variables of AC power, each of which is Gaussian distributed:

$$p_\theta(y_i) = \frac{1}{\sigma\sqrt{2\pi}} e^{-\frac{(y_i-\mu)^2}{2\sigma^2}} \tag{5.3}$$

The welding process is known to operate under either normal ($\theta = \mu_0$) or fault ($\theta = \mu_1$) conditions where $\mu_0 > \mu_1$. Furthermore, we assume that prior to $t = 0$, $\theta = \mu_0$ and it may only change to $\theta = \mu_1$ at one of the n sampling instants. Consider the problem of testing $k + 1$ hypotheses $H_0, H_1 \ldots H_k$

$$\begin{aligned} H_0: &\quad \theta = \mu_0 \quad for \quad 1 \le i \le k \\ H_j: &\quad \theta = \mu_0 \quad for \quad 1 \le i \le j-1 \\ &\quad \theta = \mu_1 \quad for \quad j \le i \le k \end{aligned} \tag{5.4}$$

If the instant of change j is fixed, then the Sequential Probability Ratio Test (SPRT) between H_0 and H_j is based on a comparison of the likelihood ratio [?]:

$$S_j^k = \sum_{i=j}^{k} s_i \tag{5.5}$$

where

$$s_i = \ln \frac{p_{\mu_1(y_i)}}{p_{\mu_0(y_i)}} \tag{5.6}$$

to a threshold h. At the sampling instant k, S_j^k is computed. If $S_j^k \ge h$ a defect in the weld joint is detected. In the scalar independent case S_j^k is recursively updated as:

$$S_j^{k+1} = S_j^k + s_i \tag{5.7}$$

In the case of a change in the mean value μ of an independent Gaussian random sequence y_k with known variance σ^2, the sufficient statistics s_i is calculated as

$$s_i = \frac{\mu_1 - \mu_0}{\sigma^2}(y_i - \frac{\mu_1 + \mu_0}{2}) \tag{5.8}$$

which we write as

$$s_i = \frac{(\mu_1 - \mu_0)^2}{\sigma^2}(y_i - \mu_0 - \frac{\nu}{2}) \tag{5.9}$$

where

$$\nu = \mu_1 - \mu_0 \tag{5.10}$$

is the change in magnitude. The SPRT is optimal with respect to the worst mean delay, when error probability for false alarms goes to zero. The instant of change j is in fact unknown, but may be estimated using the maximum likelihood principle [?], leading to the decision function and alarm instant:

$$g_k = \max_{0 \le j \le k} S_j^k \tag{5.11}$$

$$t_a = \min\{k : g_k \ge h\} \tag{5.12}$$

The algorithm has been formulated as a set of parallel SPRT's, but may equivalently be viewed as repeated SPRT or a CUSUM - type test. The connection between these alternative points of view has been investigated by [?]. The decision function g_k introduced in 5.11 becomes in repeated SPRT formulation

$$g_k = [g_{k-1} + s_i]^+ \tag{5.13}$$

and in the Gaussian case

$$g_k = [g_{k-1} + \frac{\mu_1 - \mu_0}{\sigma^2}(y_k - \frac{\mu_1 + \mu_0}{2})]^+ \tag{5.14}$$

where $(x)^+ = \sup(0, x)$. The alarm threshold h is chosen by a tradeoff between worst mean delay for detection, τ and false alarm probability α. The CUSUM algorithm is optimal when α goes to zero [?]:

$$\tau \sim \frac{\ln \alpha^{-1}}{K(\mu_1, \mu_0)} \quad when \quad \alpha \rightarrow \quad 0 \tag{5.15}$$

where

$$K(\mu_1, \mu_0) = E_{\mu_1}[\ln \frac{p_{\mu_1}(y_i)}{p_{\mu_0}(y_i)}] \tag{5.16}$$

is the Kullback information. In Gaussian case the Kullback information is

$$K(\mu_1, \mu_0) = \frac{(\mu_1 - \mu_0)^2}{\sigma^2} \tag{5.17}$$

Due to Wald's inequality the alarm threshold satisfy

$$\alpha = e^{-h} \tag{5.18}$$

and thus the alarm threshold h is easy to obtain [**?**]. The complete fault detection algorithm may be summarized as follows:

Algorithm: For each section k of 1024 data samples:

1. calculate AC power y_i
2. calculate $g_k = [g_{k-1} + s_i]$
3. **if** $g_k \leq 0$ **then** $g_k = 0$
4. **if** $g_k \geq h$ **then**
   Alarm
   $g_k = h$

Chapter 6

Evaluation and Tuning

6.1 Evaluation

In order to evaluate the proposed detector, two batches, each of 180 samples of the parameter y_i originating from weld voltage from normal welds and welds during step disturbance respectively, were used, see figure 6.1. A sample length of 184 and welding speed at 10 mm/s corresponds approximately to a 20 cm weld joint.

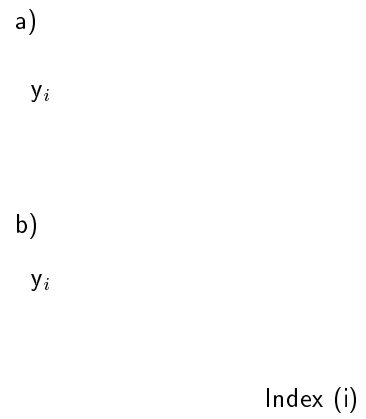

Figure 6.1: The AC power y_i during normal weld. The AC power y_i during step disturbance. The AC power y_i is based on 1024 samples of the weld voltage.

The estimated AC power of the weld voltage y_i is assumed to be identically, independent, Gaussian distributed with mean value μ_0 and μ_1 under normal and fault condition respectively. The variance σ is assumed to be constant under both conditions. For each batch of data, mean value and variance are estimated, see table 6.1.

Table 6.1: List of estimated parameters.

Estimated Parameters		
	mean value $\hat{\mu}$	variance $\hat{\sigma}^2$
Normal conditions	56.4	6.76
Fault conditions	47.2	9.10

χ^2 tests shows that the AC power y_i under fault condition, in contrast to normal conditions, is neither independent nor Gaussian. Furthermore, the variance is not equal under the both condition, see table 1. The algorithm is still chosen, because the algorithm is robust with respect to independent and Gaussian assumption as well as demand for equal variance [**?**, **?**]. In addition, storage and computational requirements for the recursive SPRT are moderate.

6.2 Tuning

In the proposed algorithm the only tuning parameter is the threshold h. Using formula 5.15 we can compute worst mean delay for detection, τ and false alarm probability α and use them for choosing a relevant alarm threshold, h. If the false alarm probability α is set at 10^{-9}, the alarm threshold h is calculated to be $h = 21$. But, since y_i under fault conditions is correlated and can not be assumed Gaussian and we assume $\sigma^2 = 6.76$, the alarm threshold h is set conservatively. Thus, in order to maintain the false alarm probability, $\alpha \geq 10^{-9}$ the alarm threshold, h is set at 25.

Chapter 7

Results

Test of the SPRT algorithm

The recursive SPRT algorithm was tested on 31 specimens. A total of 15 experiments were conducted for reference T-joint and sixteen experiments were conducted for the T-joint with step disturbance. The recording time of the measured signals was 15 s.

The test was designed as follows: When the alarm turns on and there is a step disturbance, the test results in a detection; and when the alarm does not turn on, there is a nondetection. If the alarm turns on and there is no step disturbance, the result is a false alarm.

Results

The results of the test are shown in table 2. Typical behavior for a T-joint with a step disturbance, is shown in figure 7.1. The top diagram of the figure, part a, shows the weld voltage, and part b shows the weld current. Part c shows the corresponding AC power y_i and the actual position of the step disturbance along the weld joint. Part d of the figure shows decision function g_i and the *Alarm*.

Table 7.1: The results of the test of the SPRT algorithm. Welding speed = 10 m/s

Type of T-joint	Reference	Step
Number of specimens	15	16
Detection	15	16
Nondetection	0	0
False Alarm	0	0

d)

G_K

Reference T-joint

Position (mm)

Figure 7.1: Illustration of the detection of step disturbance: Measured weld voltage and current are shown in part a and b respectively. The corresponding AC power y_i and the actual position of the step disturbance are shown in part c. The decision function g_i and $Alarm$ is shown in part d.

G_K

T-joint with step disturbance

Position (mm)

Chapter 8

Discussion

monitoring indices

arbetspunkt

The proposed recursive SPRT algorithm is designed to detect step disturbance in welds. The algorithm could, however, be used to detect other disturbances in the weld process as well. Furthermore, to enhance the performance of the algorithm, other parameters such as short-circuit time and short arc time can easily be incorporated into the algorithm.

kombinera parametrar. strom o. spaanning

tuning parameters for other experiment

tuning parameters - minimum jump